ADVANCED MATERIALS INTERFACES
www.advmatinterfaces.de

Titanium as an Instant Adhesive for Biological Soft Tissue

*Masahiro Okada, Emilio Satoshi Hara, Atsushi Yabe, Kei Okada, Yo Shibata, Yasuhiro Torii, Takayoshi Nakano, and Takuya Matsumoto**

A variety of polymer- and ceramic-based soft-tissue adhesives have been developed as alternatives to surgical sutures, yet several disadvantages regarding the mechanical properties, biocompatibility, and handling hinder their further application particularly when applied for immobilization of implantable devices. Here, it is reported that a biocompatible and tough metal, titanium (Ti), shows instant and remarkable adhesion properties after acid treatment, demonstrated by ex vivo shear adhesion tests with mouse dermal tissues. Importantly, in vivo experiments demonstrate that the acid-treated Ti can easily and stably immobilize a device implanted in the mouse subcutaneous tissue. Collectively, the acid-treated Ti is shown as a solid-state instant adhesive material for biological soft tissues, which can have diverse applications including immobilization of body-implantable devices.

The number of surgical procedures continues to grow every year,[1] although current surgical closure techniques still involve the use of invasive techniques with sutures. The suturing technique is time-consuming and highly dependent on the physician's skills, and hence often result in secondary tissue damage, microbial infection, fluid or air leakage, and poor cosmetic outcome.[2] Surgical sutures are also currently used for immobilization of body-implanted devices, such as artificial pacemakers,[3] deep brain stimulation (DBS),[4] and spinal cord stimulation (SCS)[5] devices, although the common hardware-related complications include the intrabody mobility of electrode leads[3–5] and pulse generators.[6–8] Additionally, the suturing technique is sometimes inadequate due to the patients' conditions, such as insufficient or fragile tissues,[9] and due to the type of devices (e.g., injectable small devices cannot be immobilized by suturing). An appealing option to sutures is the use of tissue adhesives.

Adhesives for soft tissues have been used since 1960.[10] The glue type adhesive spreads over the entire contact area, which eliminates stress localization facilitating load transfer between the ruptured surfaces, and hence is easy to apply, join dissimilar materials, increase design flexibility, improve cost effectiveness.[1] Currently, three main types of tissue adhesive glues have been clinically used: cyanoacrylate,[11] gelatin–resorcinol–formaldehyde,[12] and fibrin.[13] However, these current tissue adhesives still present limitations related either to biocompatibility (for cyanoacrylate and gelatin–resorcinol–formaldehyde adhesives) or bonding strength (for fibrin adhesives).[10,14] More recently, researchers have developed unique biocompatible adhesives with higher adhesive strength by using polymers[1,14–16] and ceramics.[17,18] However, polymers have limitations of their mechanical strength and ceramics show a brittle property.

Titanium (Ti), one of the metallic biomaterials, presents excellent mechanical properties compared with polymer or ceramic biomaterials, and higher biocompatibility compared with other metals.[19] Due to these characteristics, Ti has long been used as the substitution for hard tissue in the field of orthopedics and dentistry, and several kinds of surface modification methods have also been developed.[20,21] However, the application of Ti as soft tissue adhesives has never been explored. In fact, nonmodified Ti shows almost no adhesion to biological soft tissues (**Figure 1**G).

Here, we hypothesized that surface modification of Ti could provide an adhesive property for soft tissues. In this study, a grade 1 commercially pure Ti (CPTi) film with 15 μm in thickness was used as a substrate, and acid treatment with HCl/H_2SO_4 was used as the chemical modification. The acid treatment has been already used to create roughened surfaces of Ti implants,[22] and has been demonstrated to be an effective way to promote the osseointegration (i.e., bonding to hard

Dr. M. Okada, Dr. E. S. Hara, Dr. A. Yabe, Prof. T. Matsumoto
Department of Biomaterials
Graduate School of Medicine
Dentistry and Pharmaceutical Sciences
Okayama University
2-5-1 Shikata-cho, Kita-ku, Okayama 700-8558, Japan
E-mail: tmatsu@md.okayama-u.ac.jp
Dr. A. Yabe, Prof. Y. Torii
Department of Comprehensive Dentistry
Okayama University Hospital
2-5-1 Shikata-cho, Kita-ku, Okayama 700-8558, Japan
K. Okada
Department of Applied Chemistry and Biotechnology
Faculty of Engineering
Okayama University
3-1-1 Tsushimanaka, Kita-ku, Okayama 700-8530, Japan
Prof. Y. Shibata
Department of Conservative Dentistry
Division of Biomaterials and Engineering
Showa University School of Dentistry
1-5-8 Hatanodai, Shinagawa-ku, Tokyo 142-8555, Japan
Prof. T. Nakano
Division of Materials and Manufacturing Science
Graduate School of Engineering
Osaka University
2-1 Yamadaoka, Suita, Osaka 565-0871, Japan
The ORCID identification number(s) for the author(s) of this article can be found under https://doi.org/10.1002/admi.201902089.

DOI: 10.1002/admi.201902089

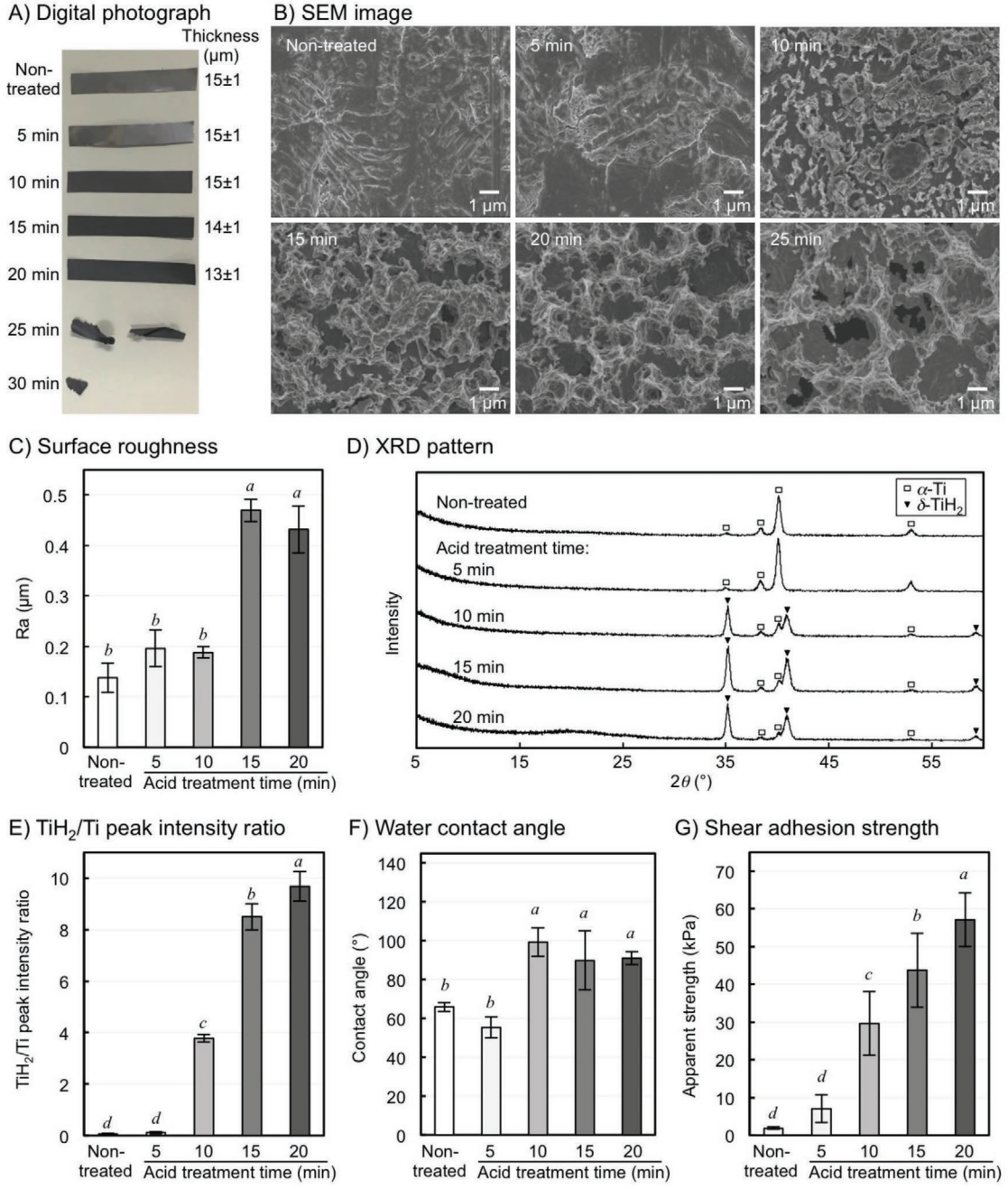

Figure 1. Surface characteristics of Ti films (thickness, 15 μm) after acid treatments. A) Digital photographs and thicknesses, B) SEM images, C) surface roughness (R_a) values, D) XRD pattern, E) XRD peak intensity ratios of TiH_2 at $2\theta = 40.9°$ and Ti at $2\theta = 38.3°$, F) water contact angles and G) apparent shear adhesion strengths of nontreated and acid-treated Ti films. The adhesion strengths were measured by ex vivo adhesion tests with mouse dermal tissues. The error bars indicate standard deviations ($N = 5$). Different italic letters (*a–d*) on bars indicate statistically significant differences between the groups in each graph, as determined by Tukey–Kramer test ($p < 0.05$).

tissues by means of increasing the interlocking capacity of Ti surface[23,24]) of bone-anchored implants. Of note, osseointegration occurs in a long term (i.e., a few months) due to the complex processes including protein adsorption, cell adhesion and cell differentiation followed by mineral precipitation onto the Ti implant surface. In this study, the instant adhesion property of acid-treated Ti film on soft tissues is reported for the first time.

The acid treatments were conducted at 70 °C for different time periods. At ≈9 min of the treatment, bubbles were formed and the solution color gradually turned into purple, indicating the dissolution of metallic Ti and the formation of H_2 gas[25] after removal of the oxidized surface layer. The acid treatment for more than 10 min markedly changed the Ti color macroscopically, and for 25 min, induced macroscopic dissolution of the film (Figure 1A).

Morphological analysis with a scanning electron microscope (SEM) revealed nanosized structures on the film surfaces after 15 min of treatment (Figure 1B; see also Figure S1 in the Supporting Information). Accordingly, the surface roughness (R_a) of the acid-treated films increased significantly after acid treatment for 15 min or longer (Figure 1C). The increase in the surface roughness would be important for soft tissue adhesion because of the mechanical interlocks with the tissues.

Crystallographic analysis (Figure 1D) revealed that the acid-treated Ti films consisted of α-Ti and δ-TiH_2, which could be formed by the reaction between Ti and H_2 generated by oxidation of Ti during acid treatment[25–27] longer than 10 min, and the peak ratio of δ-TiH_2/α-Ti increased linearly with the acid treatment time (Figure 1E). The X-ray diffraction (XRD) measurements showed no formation of crystalline TiO_2 (Figure 1D), which is in accordance with a previous study.[25,27]

Young's moduli of α-Ti and δ-TiH_{2-x} (around 63.5 at% hydrogen content) are reported to be around 105 and 40 GPa,[28] respectively, which are consistent with the flexural elastic moduli of nontreated and 20-min-treated films (see Figure S2 in the Supporting Information). The decrease in the flexural modulus after the acid treatment would be preferable to increase the film flexibility and promote a tighter contact with soft tissues,[29] especially in uneven-surfaced tissues (see Figure S3 in the Supporting Information).

The mechanical strength of the adhesive itself should be substantially larger than the target tissue, because the adhesive would otherwise break under a large stress.[18] The tensile strength of nontreated Ti used in this study (see Figure S4 in the Supporting Information) was much larger than the minimum strength of grade 1 CPTi (240 MPa) defined by an American Society for Testing and Materials (ASTM) Standard,[30] which would be due to the cold rolling process during its fabrication. The tensile strength of acid-treated Ti tends to decrease as increasing the acid treatment time. However, the tensile strength of 20-min-treated film was around 140 MPa and sufficiently larger than that of human skin tissues (28–110 MPa[31]). Of note, H_2 generation accompanying with acid treatments sometimes causes hydrogen embrittlement of Ti depending on the amount and the distribution of absorbed H_2.[32] Further analyses are necessary to clarify the distribution of hydrogen inside the acid-treated films and the degree of hydrogen embrittlement.

The water contact angle measurements showed that the Ti film surface turned hydrophobic (water contact angle > 90°; Figure 1F), which is in accordance with a previous study.[27] Of note, acid-treated Ti-based dental implants nowadays are hydrophilized after the acid treatment, and their water contact angles are close to zero.[33] However, importantly, hydrophobic surfaces show stronger adsorption of most proteins compared with hydrophilic surfaces.[34]

Indeed, when the acid-treated Ti films were placed in contact with soft tissue, it could adhere instantly by gentle pressure (i.e., within a few seconds; see Movie S1 in the Supporting Information) without time-consuming setting reactions. For quantitative analysis of the adhesiveness to soft tissue, the Ti film was attached to mouse dermal tissue and ex vivo shear adhesion tests were conducted (see Figure S5 in the Supporting Information). The apparent shear adhesion strength increased linearly and was proportional to the acid treatment time (Figure 1G), reaching the highest adhesion strength of 57 ± 7 kPa with the 20-min-treated film. By removing the surface layer from the acid-treated Ti, the adhesion strength decreased significantly (see Figure S6 in the Supporting Information), supporting the importance of the hydrophobic and nanostructured TiH_2 layer formed by the acid treatment. The ex vivo shear adhesion strength of the 20-min-treated Ti film (57 kPa) was significantly higher than that of commercially available fibrin glue (e.g., 18 kPa) measured under the same conditions,[18] and was comparable to gelatin-resorcinol-formaldehyde/glutaraldehyde glue (e.g., 48 kPa) at wet conditions.[1] Of note, a simple autoclaving at 121 °C, which usually causes denaturation of most organic polymer biomaterials, could be used to sterilize the Ti films with no effect on the adhesion properties (Figure S7 in the Supporting Information).

To elucidate the adhesion mechanism, fractographic analyses were conducted after the ex vivo shear adhesion tests with mouse dermal tissues. SEM analysis revealed that fibrous tissues (i.e., collagen fiber bundles and split collagen fibers) remained on the acid-treated Ti surface (**Figure 2**A), but not on the nontreated surface (see Figure S8 in the Supporting Information). The fibrous remnants on the acid-treated films indicate the cohesive failure of fibrous dermal tissues, indicating that the adhesion strength between the film and the tissue was relatively larger than the strength of the tissue itself. Additionally, 180° peel tests revealed the stringiness, which can also be observed with pressure-sensitive acrylic adhesives,[35] of fibrous tissues on the acid-treated Ti (see Movie S2 in the Supporting Information).

Based on the adhesion theory for pressure-sensitive adhesives,[36] it is expected that a higher adhesion strength would be observed by strengthening the tissue itself (or by applying the film onto stronger tissues) due to the reduction of cohesive failure if the sticky component spread over the adherend. As expected, further shear adhesion tests with rabbit sclera, which consists of thicker collagen fiber bundles (see Figure S9 in the Supporting Information), showed a significantly larger adhesion strength of 75 ± 11 kPa (see Figure S7 and Movie S3 in the Supporting Information), yet with a similar cohesive failure of the biological tissues.

Fourier transform infrared (FT-IR) analysis (Figure 2B) of the remnants after the ex vivo test indicated that the remnants consisted of peptides/proteins, most of which were assumed to be collagen molecules based on the SEM findings (Figure 2A). The peak intensities of ester groups and hydrophobic $-CH_3$/$-CH_2-$ groups increased in the remnants compared with the intact dermal tissue, suggesting the interaction of the acid-treated Ti surface with hydrophobic components. Meanwhile, FT-IR analysis of water in the tissues showed that the O—H band of water in the intact dermal tissue was broad (at 3000–3600 cm^{-1}; see Figure 2B), whereas that in the remnants adhered onto the film became markedly narrow (at around 3250 cm^{-1}; see also the difference spectrum drawn in Figure S10 in the Supporting Information). The narrow O—H band at around 3250 cm^{-1} would be associated with "ice-like" water, which was adsorbed on hydrophobic surfaces and oriented similar to that at the water/air interface,[37] and suggests the stress-triggered exposure of hydrophobic components in the tissue.[38] Together, one of the mechanisms for the strong adhesion strength of the acid-treated TiH_2-covered Ti film is the

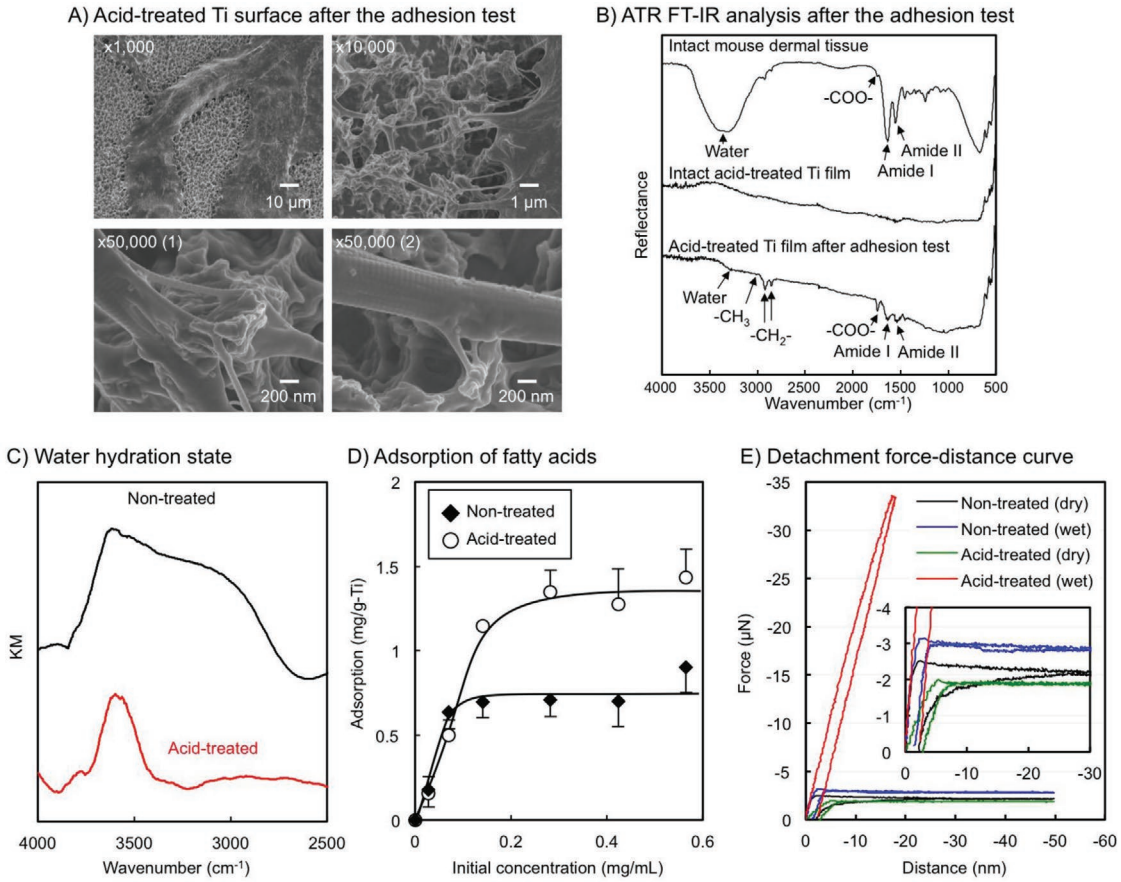

Figure 2. Comparisons between nontreated and acid-treated Ti films (treatment time, 20 min). A) SEM photographs of the acid-treated Ti film surface after the ex vivo adhesion test with different magnifications. B) ATR FT-IR spectra of intact mouse dermal tissue, and the 20-min-treated Ti film before and after the adhesion tests. Note the presence of amide, methylene and carboxyl groups on the Ti film after adhesion test, indicating the remnants of soft tissue attached to the film. C) FT-IR spectra of O—H stretching vibration of water spread on nontreated and acid-treated Ti films. D) Adsorption behaviors of oleic acid on nontreated and acid-treated Ti powders at different initial concentrations of oleic acid solution. E) Detachment force–distance curves after attaching the diamond spherical-tipped nanoindenters on nontreated or acid-treated Ti film at dry or wet state. The inlet shows the curves at the low force region.

hydrophobic interaction between TiH_2 on the film surface and hydrophobic components in the tissues.

Therefore, we compared the surface characteristics of the nontreated (i.e., nonadhering) and acid-treated Ti films in terms of hydrophobic interactions. There are currently three main theoretical approaches to modeling the hydrophobic interaction: vapor bridges models; electrostatic models; and water structure models.[38] Among them, the water structure model should be the most important in this study, because the hydrophobic interaction and biomolecule adsorption on materials are associated with the hydration state changes of the biomolecules and material surfaces.[39–41] Interestingly, the hydration layer of acid-treated Ti film was significantly different from that of nontreated Ti (Figure 2C). The hydration state of polymer biomaterials has been classified into three distinct types:[42,43] free water with almost no interaction with material surfaces; freezing-bound water (i.e., intermediate water) interacting weakly with material surfaces; and nonfreezing bound water interacting strongly with material surfaces. Particularly, intermediate water has been demonstrated to have fundamental biological importance in suppressing organic adsorption on the polymer's surface.[43,44] In the FT-IR spectra of hydrated polymers, O—H stretching vibration of water at around 3400 cm^{-1} is assigned to intermediate water.[43] The same band was observed in the FT-IR spectrum of the nontreated Ti surface, which would be covered by hydrocarbons during storage in the air,[45,46] whereas the band was negligible in the case of acid-treated Ti (Figure 2C). The peak at around 3600 cm^{-1}, which would be assigned to bound water, was observed in each Ti surface. Although the origin of the difference in the hydration structure between the nontreated and acid-treated Ti is not clear in this study, its role in organic adsorption seems to be identical with polymer materials (i.e., the solid surface with high intermediate water content would not be preferable for organic adsorption). In fact, the adsorption capacity of hydrophobic fatty acids is significantly high in acid-treated Ti compared with nontreated Ti (Figure 2D).

Next, in order to evaluate the vapor bridge model, we conducted direct measurements of detachment forces of an instrumented nanoindenter on each Ti film surface at dry or wet conditions (Figure 2E). The force required for indenter withdrawal was almost negligible in the cases of nontreated films

both at dry and wet conditions. However, in the case of acid-treated films at wet condition, the force was significantly larger (≈33 μN at a lift height of 17 nm) at a wet condition, but almost negligible at a dry condition. These results support the vapor bridges models, in which hydrophobic surfaces are prone to picking up nanoscopic air bubbles that bridge two approaching surfaces to give rise to a strong and long-range attractive capillary force.[38] Of note, the rough surface of the acid-treated film seems to be favorable to form air bubbles between the dimples.

In this study, it is not clear whether the origin of the hydrophobicity on the acid-treated Ti is due to the nature of H-terminated Ti as with hydrophobic H-terminated Si,[41] the supressed oxidation (i.e., formation of hydrophilic oxidized Ti) by absorbing reductive hydrogen, or adsorption of hydrophobic hydrocarbons[45,46] during air drying and storage after the acid treatment. Besides, it is also not clear what molecules directly adsorbed onto the acid-treated Ti after contacting with soft tissues, and the adsorbed molecules would depend on the type of soft tissue. Therefore, future study is needed to further understand the adhesion mechanism of the acid-treated Ti.

Finally, in order to demonstrate a novel function of acid-treated Ti for immobilization of medical devices, a sensor (8.0 mmW × 4.0 mmH × 2.0 mmT) attached with the acid-treated Ti was placed on the muscle fascia in vivo. The device attached with the acid-treated Ti was stably immobilized for 6 h (**Figure 3**B) and for at least 10 days (see Figures S11 in the Supporting Information), whereas the device attached with the nontreated Ti easily moved shortly within 6 h after the implantation (Figure 3A). Note that the direct and strong adhesion of the Ti film to the fascia tissue could be observed upon compulsory removal (Figure 3B, rightmost panels; see also Figure S11g in the Supporting Information). When the acid treatment was applied to the pulse generator of an artificial pacemaker, whose outer casing is usually made of Ti and size is around 5 cmϕ, the generator is expected to be immobilized without suturing in a subcutaneous tissue under a shear force lower than 22 kgf, calculated with the ex vivo shear adhesion strength (57 kPa).

In the recent advancement of Internet of Things (IoT) society, implantable devices such as microchips and biosensors have been paid great attention.[47–49] As a microchip, injectable radio frequency identification (RFID) tag[50] has now widely helped to manage livestock, domesticated or laboratory animals and products in the food supply chain. Implantable biosensors have been developing to be used not only as a monitoring system of the biorhythms,[49] but also as a drug release system for the treatment of cancers or endocrine diseases including diabetes.[51] In the near future, these implantable devices are expected to be important tools for human electronic identification, internal body monitoring and also prevention or treatment of diseases. Nevertheless, after decades of market experience with animals, the intrabody mobility (i.e., migration) of the current injectable RFID tag is still a problem.[52,53] The intrabody mobility of other implantable devices would also be one of the major problems hindering its further application. The acid-treated Ti adhesive reported here could also be useful for immobilization of the above biochips and biosensors to obtain more precise and accurate real-time information from the inner tissues or organs.

In summary, Ti showed an instant and remarkable adhesion to biological soft tissues after the acid treatment. This strategy may provide an effective method for the development of soft tissue adhesives that can potentially provide a novel platform for many practical and useful additions to the surgical apparatus.

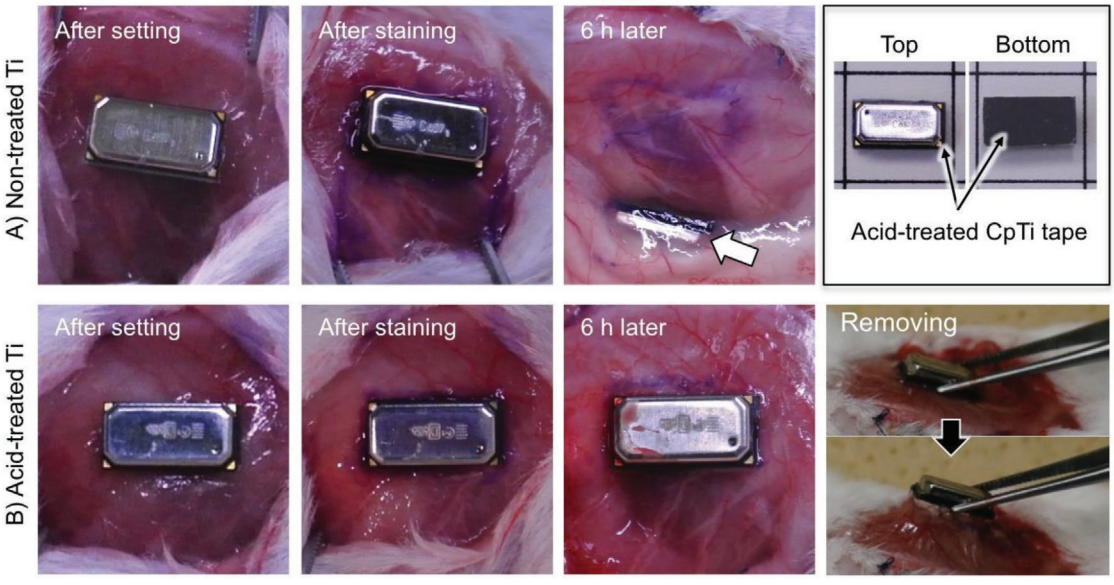

Figure 3. The sensor device attached with A) nontreated or B) acid-treated Ti film was placed on a mouse fascia. The fascia tissue around the device was stained with hematoxylin to indicate the implantation site, and then covered with the skin tissue. After 6 h, the device attached with the nontreated Ti film moved in the subcutaneous tissue, whereas the one attached with the acid-treated Ti film could be kept immobilized at the implanted site. The upper right picture shows digital photographs of the sensor device attached with the acid-treated Ti film (treatment time, 20 min). The lower right picture shows the direct and strong adhesion of the acid-treated Ti film to the fascia upon compulsory removal.

Experimental Section

Materials: Unless otherwise stated, all materials were guaranteed reagent-grade and used as received from Wako Pure Chemical Industries, Ltd. (Osaka, Japan). Milli-Q water (Millipore Corp., Bedford, MA, USA) with a specific resistance of 18.2×10^6 Ω cm was used.

Acid Treatments: A grade 1 CPTi films of 15 µm in thickness (TR2700C-H; Takeuchi Kinzokuhakuhun Kogyo Co. Ltd., Tokyo, Japan) was cut into strips (5 mm × 30 mm), washed sequentially with acetone and pure water, and dried in the air. For acid treatment, five Ti strips were immersed in an immediately mixed solution of 35 wt% HCl and 97 wt% H_2SO_4 in pure water (total amount: 10 g; final composition: 15 wt% HCl and 45 wt% H_2SO_4) in a glass tube, which was subsequently soaked in a water bath at 70 °C. After 5, 10, 15, 20, 25, or 30 min, the acid solution was aspirated, and the Ti films were washed thoroughly with pure water until complete pH neutralization. The acid-treated Ti films were then dried in the air at 60 °C for 24 h.

Basic Characterizations: The Ti surface morphology was observed by SEM (JSM-6701F, JEOL Ltd., Tokyo, Japan) operated at 5 kV after the samples were dried onto an aluminum stub and coated with osmium (Neoc-Pro, Meiwafosis Co. Ltd., Tokyo, Japan).

Product identification was conducted by thin-film XRD measurements (RINT2500HF; Rigaku Corp., Tokyo, Japan) at the incident angle of 1° using Cu-Kα (1.54 Å) irradiation at 40 kV and 200 mA. The XRD measurements were conducted from 5° to 60° at a scan speed of 1° min^{-1}. The peak intensity ratio of TiH_2 at $2\theta = 40.9°$ and Ti at $2\theta = 38.3°$ was calculated for each sample ($N = 5$) after substituting the baseline of each XRD pattern.

Tensile strengths of the Ti films were measured on a universal testing machine (Ez-test; Shimadzu Corp., Kyoto, Japan) equipped with a load cell of 500 N at a tensile rate of 0.01 mm s^{-1}. Flexural elastic moduli of the Ti films were measured by a three-point bending test at a span of 2.0 mm at a loading rate of 0.1 mm s^{-1}. The thickness of each Ti film was measured with a micrometer (MDC-25 MJ; Mitutoyo Corp., Kanagawa, Japan). Five measurements were conducted for each sample, and the average value was calculated.

The calculated average surface roughness (R_a) of each sample was determined using a profilometer (HandySurf E-35B; Mitutoyo Corp., Kanagawa, Japan) with an active tip radius of 2 µm, reading length of 1.0 mm, and reading speed of 0.6 mm s^{-1}. Five measurements at different locations, in which the distance between each parallel track set at least 0.5 mm, were recorded for each sample.

Static contact angles of water droplet in the air were measured after the droplets (10 µL) were placed on the samples surfaces. The static contact angle was calculated based on a half-angle method. Five measurements were conducted for each sample.

Nanoindentation: The nanoindentation experiments were performed using a quantitative nanomechanical testing instrument (TI 950 TriboIndenter; Hysitron, Inc., USA) interfaced with an atomic force microscope (AFM).[54] Diamond spherical-tipped indenter with a nominal indenter radius of 1 µm was chosen for this study. Force–displacement curve on the sample surfaces were recorded during the indenter tip was withdrawn from the surface to a set distance (the lift height of 50 nm) after the tip was contact on the sample surface at a preload of 2 µN. The dried films or those just after immersing in Milli-Q water were used for the nanoindentation tests. The measurements were performed five times, and a representative curve was shown.

FT-IR Measurements: FT-IR spectra were obtained using an IRAffinity-1S system (Shimadzu Corp., Kyoto, Japan) equipped with a diffuse reflectance unit (DRS-8000A; Shimadzu Corp.). First, a background spectrum was measured on the Ti sample after washing with water and drying under N_2. After the background measurement, a drop of pure water was placed onto the sample surface, and the FT-IR spectrum was recorded at a resolution of 4 cm^{-1} until the water was evaporated. The resulting diffuse reflection spectrum just before water evaporation was shown after Kubelka-Munk conversion[55] with a spectrum analysis software (LabSolutions IR version 2.13; Shimadzu Corp.). For the qualitative analysis for biological tissues on the Ti samples after the adhesion tests, the attenuated total reflectance (ATR) FT-IR spectra were recorded after pressing the samples on a ZnSe prism equipped on IRAffinity-1S (Shimadzu Corp.) with a resolution of 4 cm^{-1} at 32 scans. All the FT-IR measurements were conducted at room temperature.

Tissue Adhesion Tests: All the animal procedures undertaken in this study were strictly in accordance with the Guidelines for Animal Experiments at Okayama University after approval of the experimental protocol by Okayama University (OKU-2018797). The skin tissues were excised from the shaved back of 6 week-old female ICR mice (Japan SLC, Inc., Shizuoka, Japan) after being euthanized with CO_2 gas or an overdose of isoflurane. The dermal layer was exposed by removing fascia, trimmed into 5 mm × 40 mm strips, immersed in phosphate-buffered saline (PBS), and used within 6 h after isolation. Rabbit sclera tissues were isolated from eyeballs of a JW/CSK rabbit (male; weight, 2.6–3.0 kg) purchased from Shimizu Laboratory Supplies Co. Ltd. (Kyoto, Japan), exposed by removing conjunctiva, trimmed into 5 mm × 40 mm strips, immersed in PBS, and used within 24 h after isolation.

After the excess amount of PBS on the trimmed tissues (5 mmW × 40 mmH) was removed with filter papers, the Ti film was attached on the mouse dermal tissue (or rabbit sclera) with an overlapping area of 2 mm × 5 mm. The samples were then immediately fixed into screw-type tensile jigs (346-57262-03; Shimadzu Corp., Kyoto, Japan), whose surfaces facing the samples were covered with adhesive-backed #400 silicon carbide sandpapers (Buehler, a division of Illinois Tool Works Inc., IL, USA), on a universal testing machine (Ez-test; Shimadzu Corp.) at a speed of 150 mm min^{-1}. The apparent shear adhesion strength was calculated from the force–displacement curves by dividing the maximum load (fracture force) by the overlapping area. Five samples were examined for each test.

Implantation Tests: The nontreated or acid-treated Ti films were autoclaved, left to dry on air and attached onto the bottom side of a gyrosensor (size: 8.0 mmW, 4.0 mmH, 2.0 mmT; ENC-03RC/D, Murata Manufacturing Co. Ltd., Kyoto, Japan) with an instant glue (Aron Alpha Extra; Toagosei Co. Ltd., Tokyo, Japan). The sensors attached with the Ti films were then placed onto the fascia at the back of a 6-week-old female ICR mouse (Japan SLC, Inc.), and outlined with Mayer's hematoxylin solution (Wako Pure Chemical Industries, Ltd.) to indicate the implantation site. The skin tissue was returned to its original position and sutured. After 6 h or 10 days, the skin was reincised, and the position of the sensor was evaluated.

Statistical Analysis: One-way analysis of variance was carried out after the normality and homogeneity of variance were tested using the Shapiro-Wilk and Bartlett tests, respectively. The Tukey–Kramer test was used for intergroup comparative analysis. All statistical tests were performed using R (version 3.3.2)[56] at preset alpha levels of 0.05.

Supporting Information

Supporting Information is available from the Wiley Online Library or from the author.

Acknowledgements

The authors thank Yagishita Giken Co. Ltd. (Saitama, Japan) for supporting the fabrication of acid-treated titanium films. This work was supported partly by the Japan Society for the Promotion of Science KAKENHI (Grant Numbers: 18K09637, JP25220912, and JP25293402).

Conflict of Interest

The authors declare no conflict of interest.

Keywords

acid treatment, adhesive, hydrophobic interaction, soft tissue, titanium

Received: December 10, 2019
Revised: February 19, 2020
Published online: March 23, 2020

[1] V. Bhagat, M. L. Becker, *Biomacromolecules* **2017**, *18*, 3009.
[2] A. Lauto, D. Mawad, L. J. R. Foster, *J. Chem. Technol. Biotechnol.* **2008**, *83*, 464.
[3] M. T. Bennett, S. K. K. Tung, *J. Long-Term Eff. Med. Implants* **2010**, *20*, 187.
[4] T. Morishita, J. D. Hilliard, M. S. Okun, D. Neal, K. A. Nestor, D. Peace, A. A. Hozouri, M. R. Davidson, F. J. Bova, J. M. Sporrer, G. Oyama, K. D. Foote, *PLoS One* **2017**, *12*, 0183711.
[5] S. Eldabe, E. Buchser, R. V. Duarte, *Pain Med.* **2016**, *17*, 325.
[6] S. Koulouris, S. Pastromas, A. S. Manolis, *Europace* **2008**, *10*, 1461.
[7] J. L. Ward, T. C. Defrancesco, S. P. Tou, C. E. Atkins, E. H. Griffith, B. W. Keene, *J. Vet. Intern. Med.* **2015**, *29*, 157.
[8] I. Russi, R. Liechti, E. Memeti, S. Bertschy, V. Weberndoerfer, R. Kobza, *HeartRhythm Case Rep.* **2018**, *4*, 497.
[9] A. Dodge-Khatami, C. L. Backer, M. Meuli, R. Prêtre, M. Tomaske, C. Mavroudis, *Ann. Thoracic Surg.* **2007**, *83*, 2230.
[10] M. Matsuda, M. Inoue, T. Taguchi, *J. Bioact. Compat. Polym.* **2012**, *27*, 481.
[11] Y.-C. Tseng, H. Suong-Hyu, Y. Ikada, Y. Shimizu, K. Tamura, S. Hitomi, *J. Appl. Biomater.* **1990**, *1*, 111.
[12] S. Fukunaga, M. Karck, W. Harringer, J. Cremer, C. Rhein, A. Haverich, *Eur. J. Cardio-Thoracic Surg.* **1999**, *15*, 564.
[13] E. V Dare, M. Griffith, P. Poitras, T. Wang, G. F. Dervin, A. Giulivi, M. T. Hincke, *Tissue Eng., Part A* **2009**, *15*, 2285.
[14] J. Li, A. D. Celiz, J. Yang, Q. Yang, I. Wamala, W. Whyte, B. R. Seo, N. V. Vasilyev, J. J. Vlassak, Z. Suo, D. J. Mooney, *Science* **2017**, *357*, 378.
[15] A. Nishiguchi, Y. Kurihara, T. Taguchi, *Acta Biomater.* **2019**, *99*, 387.
[16] A. Mahdavi, L. Ferreira, C. Sundback, J. W. Nichol, E. P. Chan, D. J. D. Carter, C. J. Bettinger, S. Patanavanich, L. Chignozha, E. Ben-Joseph, A. Galakatos, H. Pryor, I. Pomerantseva, P. T. Masiakos, W. Faquin, A. Zumbuehl, S. Hong, J. Borenstein, J. Vacanti, R. Langer, J. M. Karp, *Proc. Natl. Acad. Sci. USA* **2008**, *105*, 2307.
[17] S. Rose, A. Prevoteau, P. Elzière, D. Hourdet, A. Marcellan, L. Leibler, *Nature* **2014**, *505*, 382.
[18] M. Okada, A. Nakai, E. S. Hara, T. Taguchi, T. Nakano, T. Matsumoto, *Acta Biomater.* **2017**, *57*, 404.
[19] M. Saini, Y. Singh, P. Arora, V. Arora, K. Jain, *World J. Clin. Cases* **2015**, *3*, 52.
[20] A. Palmquist, O. M. Omar, M. Esposito, J. Lausmaa, P. Thomsen, *J. R. Soc., Interface* **2010**, *7*, S515.
[21] P. Chen, T. Aso, R. Sasaki, M. Ashida, Y. Tsutsumi, H. Doi, T. Hanawa, *J. Biomed. Mater. Res., Part A* **2018**, *106*, 2735.
[22] L. Claes, S. G. Steinemann, *U.S. Patent 5456723*, **1995**.
[23] F. Butz, T. Ogawa, I. Nishimura, *Int. J. Oral Maxillofac. Implants* **2011**, *26*, 746.
[24] S. Spriano, S. Yamaguchi, F. Baino, S. Ferraris, *Acta Biomater.* **2018**, *79*, 1.
[25] N. Ren, G. Wang, H. Liu, T. Ohachi, *Mater. Res. Bull.* **2014**, *50*, 379.
[26] E. Conforto, D. Caillard, B. O. Aronsson, P. Descouts, *Eur. Cells Mater.* **2002**, *3*, 9.
[27] S. Ban, Y. Iwaya, H. Kono, H. Sato, *Dent. Mater.* **2006**, *22*, 1115.
[28] D. Setoyama, J. Matsunaga, H. Muta, M. Uno, S. Yamanaka, *J. Alloys Compd.* **2004**, *381*, 215.
[29] T. Fujie, *Polym. J.* **2016**, *48*, 773.
[30] ASTM F 67-95, *Annual Book Of ASTM Standards*, American Society For Testing And Materials, Philadelphia, PA **1995**.
[31] H. Rollhäuser, *Die zugfestigkeit der menschlichen haut. Gegenbaur. Morph. Jahrb.* **1950**, *90*, 249.
[32] D. Prando, A. Brenna, M. V. Diamanti, S. Beretta, F. Bolzoni, M. Ormellese, M. P. Pedeferri, *J. Appl. Biomater. Funct. Mater.* **2017**, *15*, 291.
[33] F. Rupp, L. Scheideier, N. Olshanska, M. De Wild, M. Wieland, J. Geis-Gerstorfer, *J. Biomed. Mater. Res., Part A* **2006**, *76A*, 323.
[34] A. Sethuraman, M. Han, R. S. Kane, G. Belfort, *Langmuir* **2004**, *20*, 7779.
[35] Y. Urahama, *J. Adhes.* **1989**, *31*, 47.
[36] *Handbook of Adhesives Technology*, 2nd ed. (A. Pizzi, K. L. Mittal), Marcel Dekker, New York **2004**.
[37] B. Torun, C. Kunze, C. Zhang, T. D. Kühne, G. Grundmeier, *Phys. Chem. Chem. Phys.* **2014**, *16*, 7377.
[38] J. N. Israelachvili, *Intermolecular and Surface Forces*, Academic Press, Cambridge, MA **2011**.
[39] W. Norde, *Macromol. Symp.* **1996**, *103*, 5.
[40] Q. Wei, T. Becherer, S. Angioletti-Uberti, J. Dzubiella, C. Wischke, A. T. Neffe, A. Lendlein, M. Ballauff, R. Haag, *Angew. Chem., Int. Ed.* **2014**, *53*, 8004.
[41] D. J. Cole, M. C. Payne, L. C. Ciacchi, *Phys. Chem. Chem. Phys.* **2009**, *11*, 11395.
[42] M. Okada, E. S. Hara, D. Kobayashi, S. Kai, K. Ogura, M. Tanaka, T. Matsumoto, *ACS Appl. Bio Mater.* **2019**, *2*, 981.
[43] M. Tanaka, T. Hayashi, S. Morita, *Polym. J.* **2013**, *45*, 701.
[44] K. Sato, S. Kobayashi, M. Kusakari, S. Watahiki, M. Oikawa, T. Hoshiba, M. Tanaka, *Macromol. Biosci.* **2015**, *15*, 1296.
[45] B. Ohler, W. Langel, *J. Phys. Chem. C* **2009**, *113*, 10189.
[46] W. Friedrichs, W. Langel, *Biointerphases* **2014**, *9*, 031006.
[47] C. Smith, *J. Technol. Manage. Innovation* **2008**, *3*, 151.
[48] H. C. Koydemir, A. Ozcan, *Annu. Rev. Anal. Chem.* **2018**, *11*, 127.
[49] M. Gray, J. Meehan, C. Ward, S. P. Langdon, I. H. Kunkler, A. Murray, D. Argyle, *Vet. J.* **2018**, *239*, 21.
[50] P. R. Troyk, *Annu. Rev. Biomed. Eng.* **1999**, *1*, 177.
[51] K. Scholten, E. Meng, *Int. J. Pharm.* **2018**, *544*, 319.
[52] ISO 15639-1, *Radio Frequency Identification of Animals - Standardization of Injection Sites for Different Animal Species - Part 1: Companion Animals (Cats and Dogs)*, **2015**.
[53] J. A. Jansen, J. P. C. M. Van Der Waerden, R. H. Gwalter, S. A. B. Van Rooy, *Vet. Rec.* **1999**, *145*, 329.
[54] N. Shimomura, R. Tanaka, Y. Shibata, Z. Zhang, Q. Li, J. Zhou, Wurihan, T. Tobe, S. Ikeda, K. Yoshikawa, Y. Shimada, T. Miyazaki, *Dent. Mater.* **2019**, *35*, 87.
[55] P. Kubelka, F. Munk, *Z. Tech. Phys.* **1931**, *12*, 593.
[56] R Development Core Team, **2016**.